Iron cycling in a mesocosm experiment in a north Patagonian fjord: Potential effect of ammonium addition by salmon aquaculture

N. Sanchez[1], M. V. Ardelan[1], N. Bizsel[2], J. L. Iriarte[3], L.M. Olsen[4]

[1] Norwegian University of Science and Technology (NTNU), Department of Chemistry, Trondheim 7491, Norway
[2] Institute of Marine Sciences and Technology, Dokuz Eylul University, H. Aliyev Bulv., No: 10, Inciralti, Izmir, Turkey
[3] Instituto de Acuicultura and Centro Dinámica de Ecosistemas Marinos de Altas Latitudes - IDEAL, Universidad Austral de Chile, Puerto Montt. COPAS Sur-Austral, Universidad de Concepción, Concepción, Chile.
[4] Norwegian Polar Institute, Fram Centre, 9296 Tromsø, Norway
Correspondence: Nicolas Sanchez (nicolas.sanchezpuerto@gmail.com)

Key words: Iron, ammonium, phytoplankton assemblage structure, particle export, fjords, salmon aquaculture

ABSTRACT

Salmon aquaculture in Chile has been a rapid growing industry, which generates increasing inputs of organic matter and inorganic nutrients into the ecosystem. We studied the potential impacts of ammonium input by this industry over the cycling of iron in a Chilean fjord. The distribution of different iron fractions at varying ammonium concentrations was monitored in a twenty-two day mesocosm experiment. The setup involved brackish and seawater; each one with Control and four ammonium concentrations. Measurements were performed for total (TFe_{Ch}) and dissolved (DFe_{Ch}) chelex labile iron fractions, and particulate (PFe) iron. Results for both brackish and seawater showed similar trends but differences in magnitude. Over time, DFe_{Ch} decreased with increasing ammonium concentration, while TFe_{Ch} showed up to a three-fold increase positively correlated to ammonium addition, chlorophyll and particulate organic carbon. Absolute PFe values also followed an increasing trend over time, with ~60 % of this fraction estimated to be of lithogenic origin. When normalized to particulate organic carbon and chlorophyll, PFe was negatively correlated to ammonium showing exponential decrease. PFe measured in 20-140 µm fraction, showed hyperbolic relation with particulate phosphorus, suggesting a change in ratio for these elements. The increase and domination of diatoms over time in both water types, together with the PFe trend observed, suggest large

phytoplankton as main driver for potential scavenged iron via available surface of the sinking cells. Positively correlated changes observed in TFe_{Ch} to changes in chlorophyll and particulate organic carbon, suggest a biological role over the particulate Fe labile fraction, hence determining potential increase of bioavailable iron. Increasing ammonium addition in the fjords of Chile caused by salmon aquaculture, may affect the phytoplankton assemblage composition and therefore the PFe to organic carbon ratio. Possible changes in biogeochemical cycling of iron, may come via nutrient enhanced diatom-dominated blooms as more efficient vectors for downward export of organic matter.

1. INTRODUCTION

The fjord ecosystem in Chile constitutes a nearly pristine environment. However, it is experiencing growing anthropogenic influence, mainly from aquaculture. The aquaculture industry has increased in the last two decades, causing growing concerns about its impact on the environment. Salmon aquaculture releases to the water column nutrients mainly as dissolved inorganic components (ammonium and phosphate) through excretion and particulate organic components (particulate nitrogen and phosphorus) through fish feces (Olsen and Olsen, 2008). Oxygen depletion and decreased biodiversity are known effects for marine sediments and benthic fauna. While consequences for benthic ecosystems from aquaculture activities are well documented (Buschmann et al., 2006, Strain and Hargrave, 2005, Soto and Norambuena, 2004), knowledge about how extra nutrient input by the industry affects structure and functions of the pelagic ecosystem is still scarce (Cloern, 2001, Olsen et al., 2006, Olsen et al., 2008). This anthropogenic input of nutrients have potential to alter the stoichiometry in seawater and therefore to some extent affect biogeochemical cycling (Arrigo, 2005) on a regional basis.

Major biogeochemical cycles in marine environment, such as carbon, nitrogen and phosphorus, strongly depend on marine phytoplankton. This group is directly responsible for approximately half of earth's primary production (Field et al., 1998). In the same way, trace elements such as Mn, Fe, Co, Ni, Cu, Zn and Cd are involved in several biological processes that are capable of influencing the major biogeochemical cycles in aquatic systems (Morel and Price, 2003). As most of these trace elements are continuously exported out of photic zone into deeper water with settling organic biomass, biological processes (uptake, trophic transfer, regeneration, excretion and decomposition) are critical in controlling the fate of these bioactive metals in the ocean (Wang et al., 2001). This highlights the feedback control

between the so-called “macro-” and “micro-” nutrients. In Chilean fjords, nitrogen is mainly contributed as nitrate (NO_3^-) by vertical entrainment of nutrient-rich Sub-Antarctic Water (SAAW) from adjacent oceanic areas (Silva et al., 1998, Silva and Prego, 2002). During assimilation by phytoplankton, NO_3^- follows a series of metabolic processes to be reduced to NH_4^+, which requires availability of Fe. Specifically within the nitrogen cycle, Fe is required as an enzyme cofactor in multiple steps, from N_2 fixation by diazotrophs to NO_3^- uptake by diatoms through sequential reduction to NO_2^- and NH_4^+ (Morel and Price, 2003).

In a setting such as Chilean fjords, it can be expected that aquaculture activities may contribute to a species shift in the macronutrient load, through increased input of dissolved inorganic macronutrients (NH_4^+ and PO_4^{3-}). The following changes may affect the phytoplankton community structure (Olsen et al., 2008, Olsen et al., 2014) and hence the long-term cycling of trace elements such as Fe. The general response of marine pelagic ecosystems to nutrient enrichment is reflected by increased nutrient uptake by phytoplankton and bacteria, with increased consequent autotrophic biomass transfer to higher trophic levels (Olsen and Olsen 2008). However, knowledge about capacity of phytoplankton to biologically uptake and metabolize this nutrient surplus is still scarce. Considering the relevance of Fe bioavailability in nitrogen cycling, we followed the changes occurred in different Fe fractions in seawater in a mesocosm experiment simulating a NO_3^- to NH_4^+ shift achieved through progressive nutrient addition over time. We assessed the feedbacks between nitrogen and iron cycling and potential implications of stoichiometry changes of these elements for phytoplankton assemblage structure in waters in the region.

2. MATERIALS AND METHODS

2.1 Study Area

Experiments were carried out during the austral summer season between 23rd of January and 14th of February 2011 at the facilities of the Huinay Scientific Field Station (42°22’46”S – 72°25’12” W) in the Comau Fjord, Northern Patagonia (Fig. 1). The fjord is orientated north south, with a maximum depth of nearly 500 m and a width of 2-8.5 km. Its hydrography features a two-layer system with the presence of a permanent low salinity layer (LSL) between the surface and ~5 m, product of the mixing of freshwater (precipitation and river runoff) with oceanic water. During the year, salinity ranges from 18 to 28 in the upper 10 m (surface water) of the water column and from 29 to 32 below the pycnocline (deeper water) (Sánchez et al., 2011). Dissolved oxygen ranges from 334.9 µmol L^{-1} in surface waters to

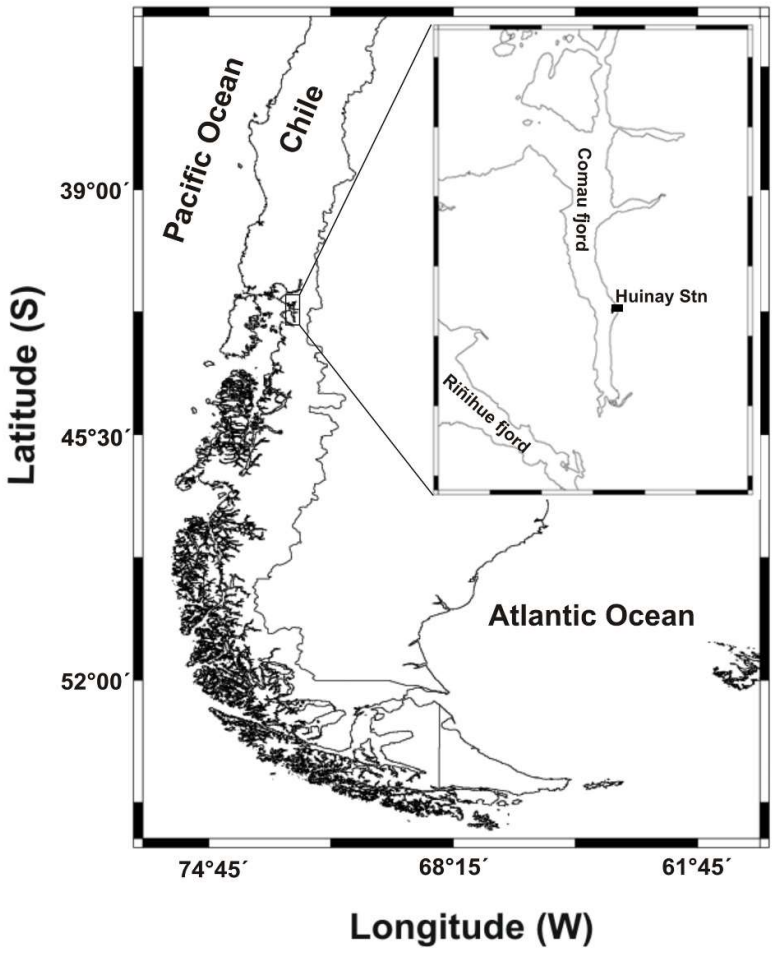

Figure 1. Study area, sampling site (Huinay Stn) and deployment of the containers for the mesocosm experiment in the Comau Fjord, Chile during January-February 2011.

183.4 µmol L^{-1} at 20 m (Jantzen et al., 2013, Pickard, 1971, Sánchez et al., 2011, Häussermann and Försterra, 2009, Iriarte et al., 2013). The sharp salinity gradient between surface and deeper water was the reason for using two water types in the experiment.

2.2 Mesocosm setup and sampling

A total of 10 (1 m^3) transparent polyethylene (PE) containers (5 mm wall thickness) were filled with fjord water. For five of them, water was collected at 2 m depth (brackish) and for the other five at 10 m (seawater). Each of the containers represented one treatment within each type of water. Except for the containers, all materials used were acid-washed in ultra-pure HNO_3 (double quartz distilled from reagent grade). The containers were thoroughly washed with the ambient seawater and preconditioned by the same seawater for one day. Water pumped into the containers was collected with a peristaltic pump (Multifix type M80), placed in a pier and using a plastic hose (35 mm diameter) placed 30 m offshore. The bottom depth at the sampling point was ca. 40 m. Water was pumped by a Watson Marlow peristaltic pump (Varmeca, 621VI) into a 30 L mixing carboy and then distributed simultaneously to all mesocosm containers by gravity-fed pipe flow. The water was not prescreened, so that it contained all different taxonomic groups at various trophic levels of the natural plankton assemblage. The experiment was conducted for 22 days and sampling was performed every third day. The containers were made into two arrays of 5-units, connected to a mooring anchored ~60 m off the coast, where the tanks partially drifted with currents. For each sampling, the array was released off the mooring and was pulled by boat to the pier. By the time the containers were pulled in, they were already mixed, but before sampling each container was mixed properly. A silicon tube (always kept packed in plastic) connected to a peristaltic pump, was introduced to reach mid-water level, from where a volume of 2-3 L was collected into PE bottles and taken to laboratory for processing (Table 1).

The containers remained closed at all times except during sampling. Initial nutrient concentrations for all treatments corresponded to those in the water collected by the peristaltic pump at the respective depths for brackish and seawater before starting the experiment. Together with each sampling for trace metals, volumes from 50 to 500 ml were collected to measure particulate organic carbon (POC), and Chlorophyll-a (Chl-a) (Parsons and Lalli, 1984). Samples (~200 mL) to determine the abundance of the main phytoplankton groups were fixed with lugol (~0.5%) for inverted microscope analysis (Uthermohl, 1958). The light transmission through the tank's walls for PAR irradiance was approximately 50%

Table 1. Date, sampling day (Sday), mesocosm, iron fractions: total chelex labile (TFe_{Ch}), dissolved chelex labile (DFe_{Ch}) and particulate (PFe) iron and other parameters measured: particulate organic carbon (POC), Chlorophyll-a (Chla), pH and phytoplankton abundance (Phy), for the different experimental treatments. * Dates correspond to the size fractionated PFe.

Date	Sday	Mesocosm	Fe Fractions	Parameters
23 / 24.01.2011	1	Seawater / Brackish	TFe_{Ch} - DFe_{Ch}	POC-Chla-pH-Phy
26 / 27.01.2011	2	Seawater / Brackish	TFe_{Ch} - DFe_{Ch} - PFe	POC-Chla-pH-Phy
29 / 30.01.2011	3	Seawater / Brackish	TFe_{Ch} - DFe_{Ch} - PFe*	POC-Chla-pH-Phy
01 / 02.02.2011	4	Seawater / Brackish	TFe_{Ch} - DFe_{Ch} - PFe	POC-Chla-pH-Phy
04 / 05.02.2011	5	Seawater / Brackish	TFe_{Ch} - DFe_{Ch} - PFe*	POC-Chla-pH-Phy
07 / 08.02.2011	6	Seawater / Brackish	PFe	POC-Chla-pH-Phy
10 / 11.02.2011	7	Seawater / Brackish	PFe	POC-Chla-pH
13 / 14.02.2011	8	Seawater / Brackish	TFe_{Ch} - DFe_{Ch} - PFe*	POC-Chla-pH

of the exterior value. Irradiance in the wavelength band 400-700 nm, i.e. photosynthetically active radiation (PAR) measured in the sea at the experiment location at the surface ranged 500 to >1500 µmol photons $m^{-2}s^{-1}$ per day depending on cloud cover. It can be estimated that the mean irradiance could reach at midday ~1000 µmol photons $m^{-2}s^{-1}$. Minimum or no UV passed through PE walls of the containers.

2.3 Nutrient additions

In order to simulate nutrient enrichment occurring in natural water, containers were supplied with four different concentrations (treatments) of macronutrients (nitrogen, phosphorus and silicon) in the form of ammonium chloride (NH_4Cl), sodium dihydrogen phosphate monohydrate ($NaH_2PO_4 \cdot H_2O$) and sodium metasilicate nonahydrate ($Na_2SiO_3 \cdot 9 \cdot H_2O$). Additions were made every third day throughout the experiment (Table 2). Although silicon is not added to the environment by aquaculture industry, it was supplied to the containers as fjord ecosystem in southern Chile has continuous and in excess natural riverine input of it, thus preventing potential nutrient limitation for diatoms. At start of the experiment, water in the upper column had a very low concentration of nitrogen, as can be the situation when nutrients are exhausted at the end of spring bloom (Magazzù et al., 1996, Iriarte et al., 2001). Notwithstanding, nutrient additions were conducted based on average ratios occurring in the area (González et al., 2010, González et al., 2011, Iriarte et al., 2013). The five treatments used for each water type, were denominated as Control, Natural, Conc 1, Conc 2 and Conc 3, where "Control" corresponded to the unit with no addition of nutrients, whereas "Natural", received a nutrient input at Redfield ratio for N:P:Si (Redfield, 1958). The three other units received experimental nutrient concentrations from the lowest (Conc 1) to the highest (Conc 3) (Table 2). All macronutrient solutions were prepared from reagent grade and treated by adding chelex-100 resin (Bio-Rad Laboratories) to remove iron and other trace elements from solution (see Section 2.5). Solutions were collected in acid-washed PE bottles.

2.4 Laboratory work

Processing of samples collected in field was performed under Class-100 laminar flow hood (Air Clean-600 PCR Workstation). The laboratory work was carried out in a class 1000 clean laboratory (Department of Chemistry-NTNU). After processing, all Fe samples were analyzed by High Resolution Inductive Coupled Plasma Mass Spectrometry (HR-ICP-MS) Element 2 (Thermo-Finnigan) with PFA-Schott type spray chamber and nebulizer.

Table 2. Concentrations (µM) of macronutrients added as NH_4Cl for nitrogen (N), $NaH_2PO4{\cdot}H_2O$ for phosphorus (P) and $Na_2SiO_3.9H_2O$ for silicon (Si) in the different treatments for brackish (6 to10) and seawater (1 to 5) mesocosms. Values corresponded to the final concentrations reached by daily partial additions. Control units had no nutrient addition; values corresponds to the concentration measured at day 0, for brackish (6-10) and seawater (1-5) treatments respectively.

Treatment	Mesocosm	N	P	Si
Control	1 and 6	0,3-0,3	0,51-0,23	6,0-4,5
Natural	2 and 7	6,5	0,4	3,2
Conc 1	3 and 8	26,4	1,1	13,1
Conc 2	4 and 9	65,8	2,7	32,6
Conc 3	5 and 10	102,8	4,3	51,0

2.5 Total and dissolved labile iron

Samples for total chelex labile (TFe_{Ch}) and dissolved chelex labile (DFe_{Ch}) iron (free metal ions and kinetically labile forms) were collected in acid-washed PE bottles. A volume of water (~150 mL) was collected and 0.8 mL (~0.4 g dry weight resin) of chelex-100 slurry (Bio-Rad Laboratories) was added. Before addition to water samples, the chelating ion-exchange resin was acid washed (2-3 M ultra-pure HNO_3) for 2 hours and rinsed twice with 18.2 MΩ-deionized (DI) water. Then ~500 µL 13.5 M ammonia solution (Suprapur Merck) was added to maintain in ammonium form. For DFe_{Ch}, water was filtered through 0.2 µm acid washed filters (0.45 + 0.2 µm Sartorious Sartobran 300) using all-plastic syringes (PE). The DFe fraction was defined operationally by 0.2 µm nominal pore size filter and therefore include colloidal Fe and does not correspond to the truly dissolved iron (de Baar and de Jong, 2001). All samples were double-bagged and placed in a shaker (65 – 80 rpm) for 48 – 72 hours. After this period, each sample was poured into a PE funnel attached to an acid-washed Poly-prep Chromatography column with a built-in polyethylene frit (pore size 100– 300 µm size) (Bio-Rad Laboratories). The water was washed through and the chelex-100 resin binding metals was retained in the frit. Each column was first rinsed with DI water and secondly with~10 mL of 0.1 M ammonium acetate buffer (pH: 9.6) to completely remove the seawater matrix. The buffer was prepared from 13.5 M ammonia (suprapur Merck) and 17.4 M acetic acid (trace ultra Fluka). The labile fractions (dissolved and particulate) presented, are based on iminodiacetic acid tridentate ligand capacity of the ion exchange resin Chelex-100 at natural pH of seawater and therefore it does not include the acid leachable fraction. Samples where packed and stored at 4˚C until transport back to NTNU facilities. Extraction of trace metals was done in a two-step acidification process, obtaining a final 5 mL 0.6 M HNO_3 sample (Ardelan et al., 2010, Öztürk et al., 2002).

2.6 Particulate iron (PFe)

Total and size-fractionated filtration was performed to determine concentration and distribution of the total particulate iron and that in different size fractions. The particulate fraction is also operationally defined by the matter retained on a 0.2 µm nominal pore size filter. The measurements for total and size-fractionated filtration were carried out in sequential and not on parallel sampling days (Sday) (Table 1). For total PFe, filtration was performed through 0.2 µm (47 mm diameter) filters, while size-fractionated filtration, encompassed a range of four size-classes (20 – 140 µm, 10 – 20 µm, 2 –10 µm and 0.2 – 2 µm) representing the main biological functional groups present in plankton community. For

20 –140 μm fraction, filtration was performed with acid-washed meshes (Nitex). The water was first prescreened (140 μm mesh) and the material retained on the 20μm mesh was then washed on 0.2 μm filters. Subsequent filtration (>10 - >2 ->0.2 μm fractions) was performed by collecting the water from the previous filtrate with a simple filtration system fitted to a peristaltic pump and using acid washed filters (isopore membrane, polycarbonate, hydrophilic, 10, 2 and 0.2 μm pore size; 47 mm diameter). For the purpose of analysis of data, PFe fractions of 2 – 10 μm and 10 – 20 μm were merged in the 2 – 20 μm fraction. Filtration volumes ranged from ≥ 2000 mL for larger fractions to 100 mL for smaller ones. Samples were kept frozen until further processing. For dates when size-fractionated data were collected, all values per each filter size were added to obtain "total PFe" in order to compare to the observed trend over time in PFe. Within the samples, Particulate aluminum (PAl) and particulate phosphorus (PP) were also measured. Since no fractionated POC data was available, PP was used to normalize size-fractionated data for PFe. In the clean laboratory, samples underwent High Performance Microwave Reactor (Ultra Clave UC Milestone) digestion, by placing the filters into Teflon tubes, adding 5 mL of 7 M ultra-pure HNO_3 and then placing filters inside the UC for two hours. After digestion, samples were diluted to 61 ± 0.3 mL with DI water to reach a final 0.6 M HNO_3 concentration. Final particulate element concentrations were calculated for each fraction based on filtered volume and dilution factor.

2.7 Blanks, standards and detection limits

The detection limit used here is three times the standard deviation of measured method blank values. Table 3 shows method blanks and detection limits for HR-ICP-MS analyses. The method accuracy for total and dissolved chelex labile samples was determined by extraction of certified seawater reference material for trace metal NASS-6, from the National Research Council of Canada (NRC), with a mass Fe concentration of 0,495 ± 0,046 $\mu g.L^{-1}$. The incomplete recovery, most likely reflect loss of transferred material from bottle to column, during extraction procedure. For particulate samples, it was used a certified reference material for tea (Oriental-Basma Tobacco) leaves (GBW-07605) from the Institute of Nuclear Chemistry and Technology Warzawa-Poland.

Table 3. Absolute values (nmol), standard deviation (SD), relative standard deviation (RSD: %) of the method blank for determination of the Fe chelex labile fractions and the filter blanks for the particulate samples for Fe, Al and P. Concentration for the reference materials NASS-6 (nM) for the chelex labile fractions and for the tea leaves GBW-07605 ($\mu g.g^{-1}$) for the particulate fraction. Percentage of recovery (Rec: %) for the reference material for each element. *Method blanks: 20 ml deionized water (18.2 MΩ) water +10 ml ammonium acetate solution treated exactly as sample with 0.8 ml clean chelex-100 and eluted similarly with pre-concentration factor of 30.

Blank		**n**	**nmol**	**SD**	**RSD (%)**	**Rec (%)**
Method blank*		8	0,08	0,02	28,6	
Standard NASS-6			**nM**			
Fe		16	8,8	0,6	8,5	85
Particulate	**Filter (µm)**		**nmol**			
Fe	0,2	3	0,09	0,02	24,3	
	2	3	0,07	0,01	11,1	
	10	3	0,07	0,04	50,5	
Al	0,2	3	0,44	0,21	48,7	
	2	3	0,23	0,02	9,9	
	10	3	0,59	0,33	55,5	
P	0,2	3	0,43	0,09	21,0	
	2	3	0,49	0,15	30,1	
	10	3	0,46	0,08	17,9	
Standard GBW-07605			**$\mu g.g^{-1}$**			
Fe		9	264			99
Al		9	3000,0			89
P		9	2840,0			106

3. RESULTS

3.1 Total and dissolved labile iron

Measurements for TFe_{Ch} and DFe_{Ch} during the experiment showed high variability between treatments and water type, with overall higher TFe_{Ch} and DFe_{Ch} concentrations in seawater compared to brackish treatments (Fig. 2). Mean TFe_{Ch} concentrations in Control and Natural in both water type showed lowest values among all treatments. TFe_{Ch} distribution in every treatment in both water type followed the same pattern over time but different in magnitude: an initial increase followed by a maximum and a posterior decline. This pattern was also followed by POC, Chl-a, pH, and phytoplankton abundance in each water type (Fig. 2 and Fig. 3). TFe_{Ch} increase in treatments with NH_4^+ was at least two-fold compared to Controls in both water types. TFe_{Ch} in Conc 2 and Conc 3 reached similar maximum values in brackish water, while it decreased in Conc 3 relative to Conc 2 in seawater. Overall, TFe_{Ch} were positively correlated to NH_4^+ addition in both brackish and seawater, whereas DFe_{Ch} exhibited the opposite trend, but with no significance (Fig 4). DFe_{Ch} distribution showed less variability than TFe_{Ch}, and except for Control in seawater, final concentrations for all treatments in both water types were lower than initial ones. DFe_{Ch} in treatments with enhanced NH_4^+ addition in brackish water, showed declines over time from 44% in Conc 1 to 67% in Conc 3, relative to Natural treatment. DFe_{Ch} in seawater showed the same trend with 43, 52 and 54% decline in concentrations in Natural, Conc 1 and Conc 2 treatments, respectively. Decrease in Conc 3 (41 %) was smaller than in Conc 2.

3.2 Particulate iron (PFe)

Initial concentrations of total PFe (Sday 2) ranged from 45 to 66 nM in brackish and seawater. Average concentrations in seawater were higher (93 ± 28 nM) than in brackish (76 ± 22 nM). Like TFe_{Ch}, PFe trend showed proportional increase to NH_4^+ addition. Average increases represented 37 and 68% in brackish and seawater respectively, compared to initial values (Fig. 3a and Fig. 3c). However, when normalized to Chl-a (data not shown) and POC (PFe:POC), the PFe trend inverted (Fig. 3e). Normalized PFe values plotted against Chl-a and POC for the three NH_4^+ addition treatments, showed exponential decay (R^2 values 0.51 to 0.96) (Fig. 5).

PFe values obtained from size-fractionated filtration, i.e. the three PFe size-fractions merged, followed the same increasing trend as total PFe in both brackish and seawater. Yet, the three values obtained in each water type were consistently above the values observed for total PFe

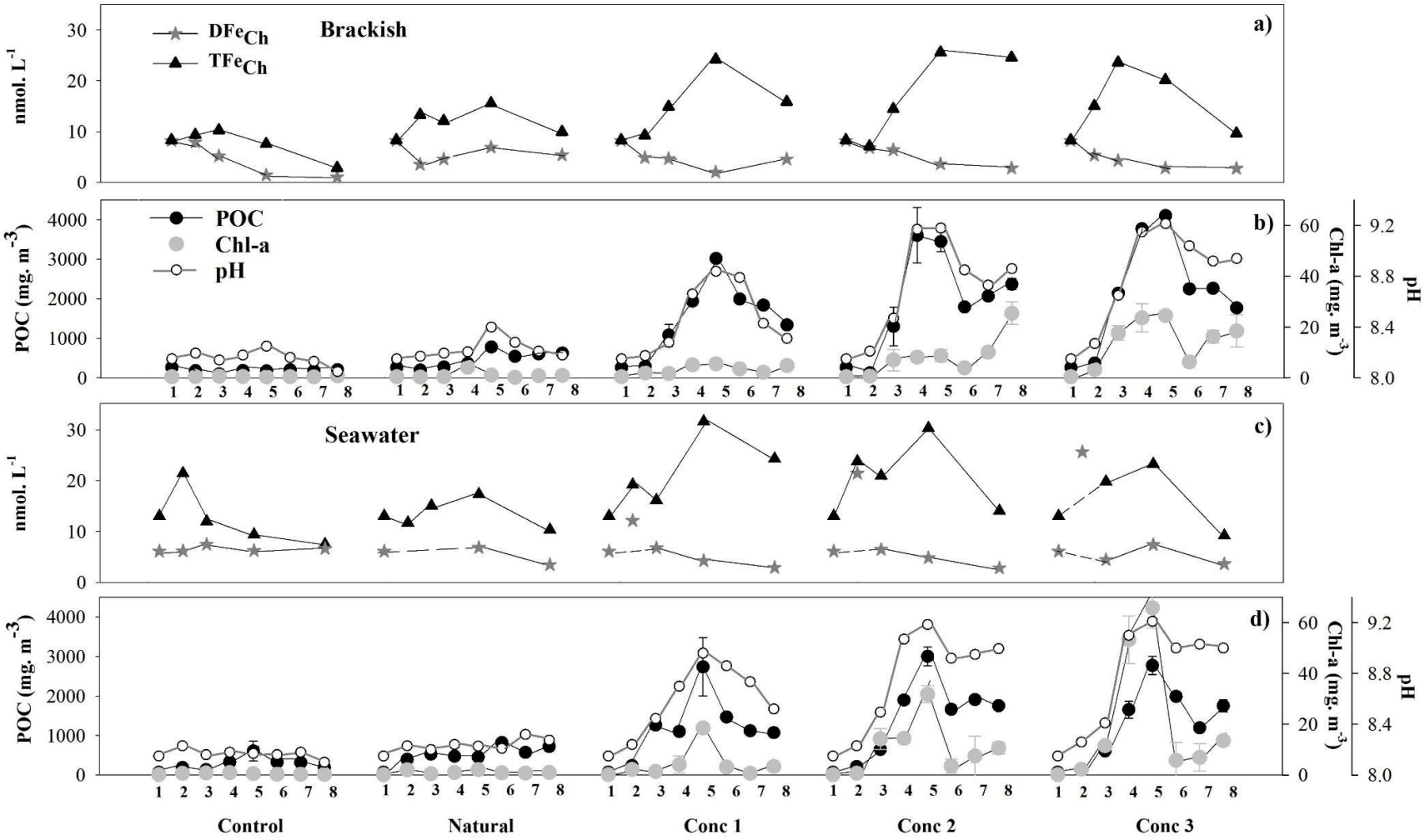

Figure 2. Total chelex labile iron (TFe_{Ch}), dissolved chelex labile iron (DFe_{Ch}), Chlorophyll (Chl-a) (µg L^{-1}) (Right axis), particulate organic carbon (POC) (µg L^{-1}) (Left axis) concentrations and pH (Right axis) in the a) - b) brackish and c) - d) seawater mesocosms for all treatments. Isolated points: Data with DFe_{Ch} at the level or above $TFe_{Ch,}$ considered contamination outliers. Dash line: missing data. Error bars: standard deviation (n=3).

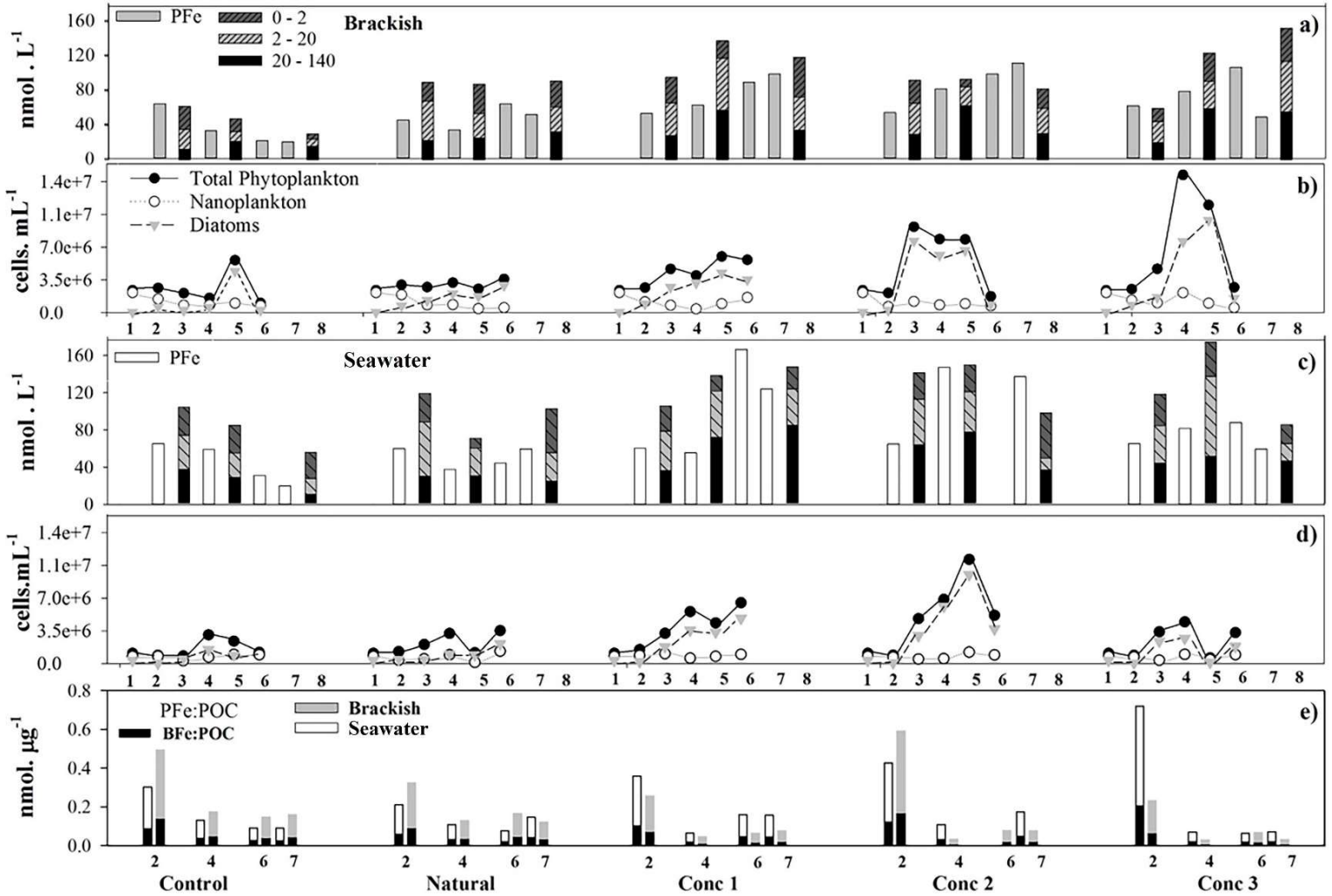

Figure 3. Distribution of PFe (nM) and abundance (cell L^{-1}) of phytoplankton: total, diatoms and nanoplankton in a) - b) brackish and c) - d) seawater mesocosms. For Sday 3, 5 and 8 PFe corresponded to size-fractionated data (added fractions in three different size-class filters (µm). e) PFe normalized to POC (nmol µgr^{-1}) (PFe:POC), for all treatments along time in brackish and seawater mesocosms. Black bars: estimated PFe biogenic fraction (BFe:POC).

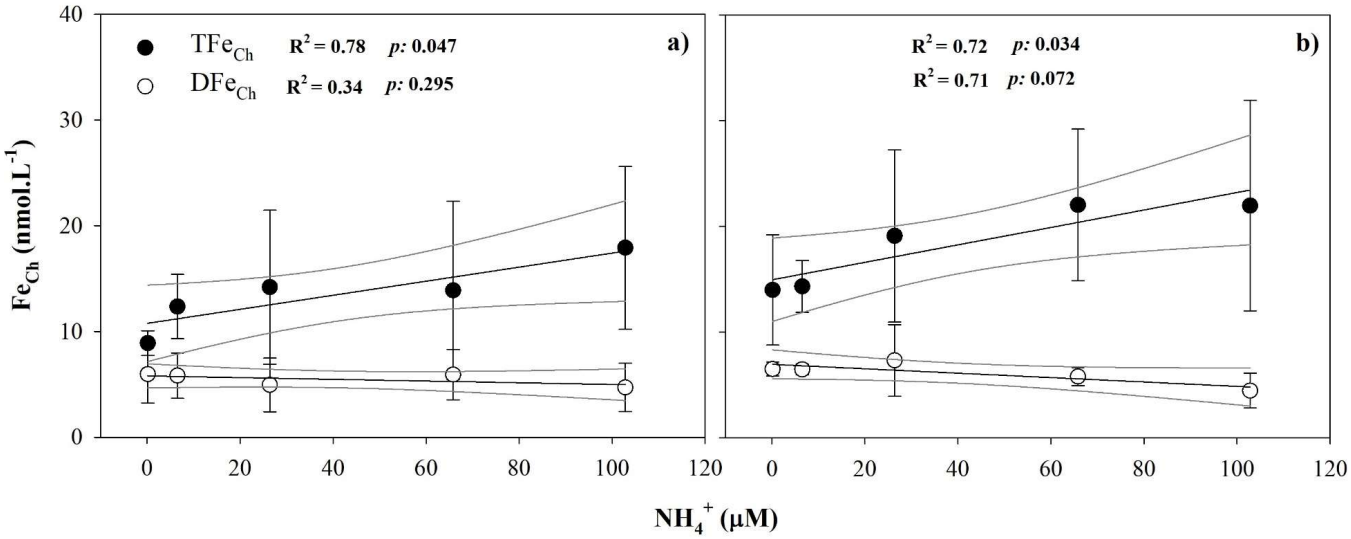

Figure 4. TFe_{Ch} and DFe_{Ch} correlation to NH_4^+ concentration for the a) brackish and b) seawater mesocosms, for all experimental treatments. Error bars: standard deviation (n=5).

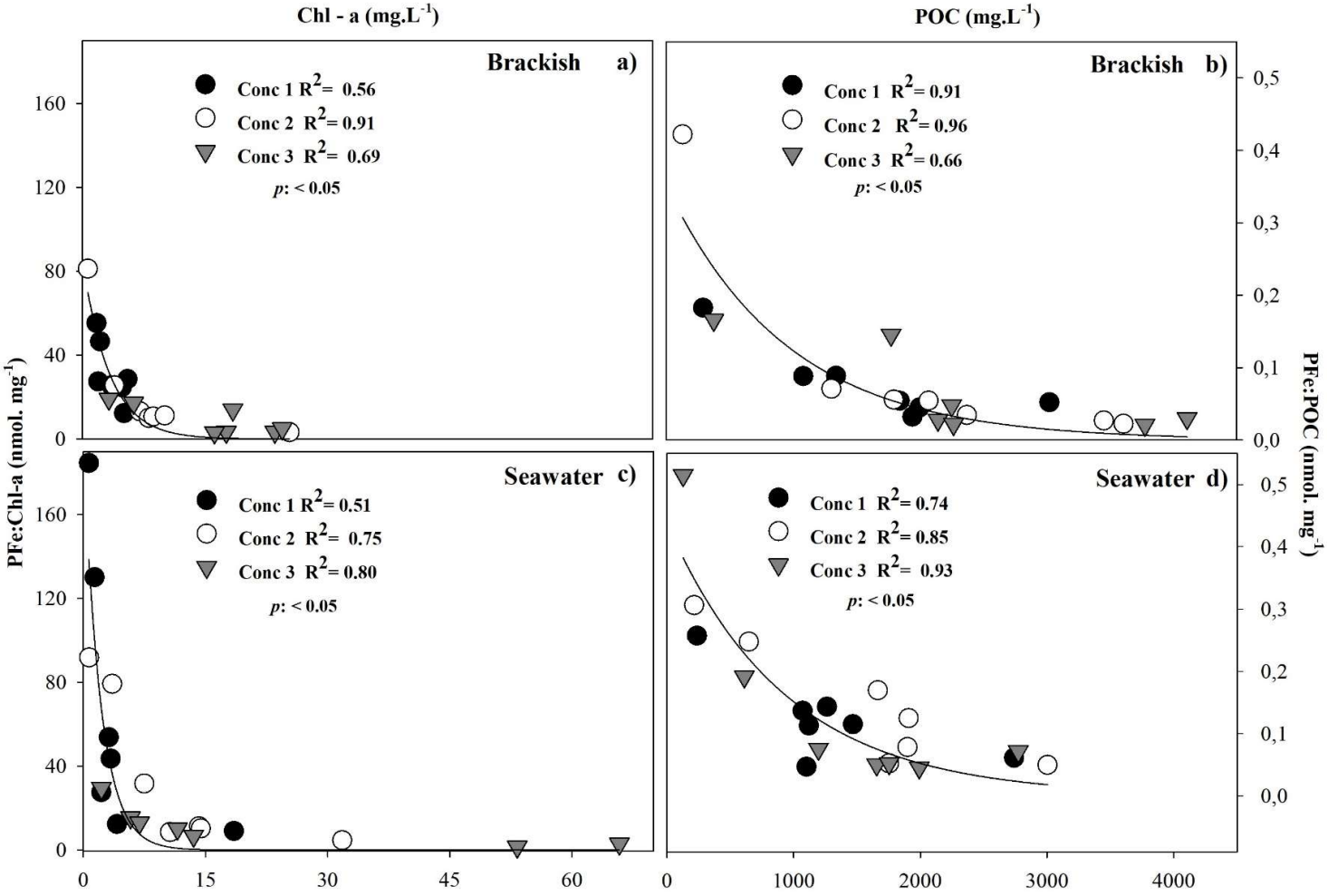

Figure 5. PFe normalized to Chl-a (nmol μg^{-1}) and to POC versus Chl-a ($\mu g\ L^{-1}$) and POC ($\mu g\ L^{-1}$) in the a) - b) brackish and c) – d) seawater mesocosms, for treatments with enhanced nutrient addition (Conc 1, Conc 2 and Conc 3).

252 over the time course (Fig. 3a and Fig. 3c). Control PFe values -obtained from size-fraction
253 filtration- in both brackish and seawater, showed a consistent decrease over time, while
254 values in all treatments with NH_4^+ addition showed overall increase. Within individual PFe
255 fractions, mean values in seawater treatments presented larger variability than brackish ones
256 (Fig. 6). In general, PFe in 0.2-2 and 2-20 µm fractions presented slight tendency to decrease
257 with increased NH_4^+ addition on brackish water. On the contrary, PFe in 20-140 µm fraction
258 increased proportional to NH_4^+ addition, accounting for larger proportion of total PFe in both
259 types of water by the end of experiment. Increase in PFe in 20-140 µm fraction in seawater
260 was ~ two-fold relative to Control and Natural treatments, but only in Con1 and Conc 2. PFe
261 size-fractionated data showed changes in the ratios with the particulate fractions of
262 macronutrients phosphorus (PP) and silicon (PSi). PFe:PP and PFe:PSi in the 20-140 µm
263 fraction in brackish and seawater, showed a hyperbolic relation with increasing macronutrient
264 concentration. This contrasted with the constant PSi:PP ratio in the same fraction (Fig. 7).

265 **3.3 Phytoplankton assemblages**

266 Average phytoplankton abundance was higher in brackish than in seawater. The trend over
267 time showed an increase in abundance proportional to NH_4^+ addition in both types of water
268 (Fig. 3b and Fig. 3d). The abundance among main groups revealed initial high values and
269 dominance of nanoplankton in brackish water (> 2 x 10^6 cells mL^{-1}), whereas both diatoms
270 and nanoplankton were present in relatively low numbers (~3 - 7 x 10^5 cells mL^{-1}) in
271 seawater. In brackish water, nanoplankton abundance declined over time with relatively low
272 values in all treatments except some peaks. In seawater, nanoplankton abundance remained
273 low throughout the experiment in all treatments. Diatoms in contrast, grew steadily in
274 treatments with NH_4^+ addition, until abrupt decline, in both brackish and seawater. No
275 correlation was found between diatom composition and water type over time, and general
276 dominance of chain-forming centric diatoms such as *Chaetoceros* spp. (medium and small
277 sizes) and *Guinardia delicatula* was observed. By middle of the experiment, medium sized
278 *Chaetoceros* spp. represented >70% in all treatments, both in brackish and seawater.
279 Generally, the abundance pattern of the main phytoplankton groups followed the observed
280 changes in PFe fractions.

281 **4. DISCUSSION**

282 On a broad perspective the variability observed in biological and physico-chemical
283 parameters measured over time in both types of water, was determined primarily by the

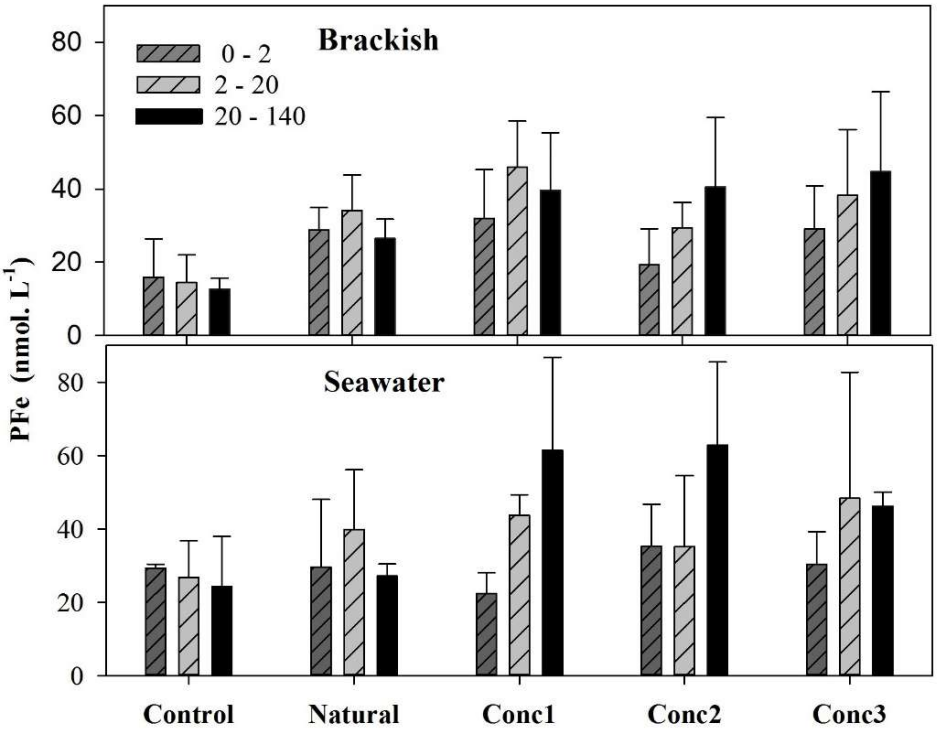

Figure 6. Distribution of the PFe size-fractionated data (nM), within each of the three different size-class filters (μm) for Sday 3, 5 and 8 in the brackish and seawater mesocosms. Error bars: standard deviation (n=3) of the mean of the three measurements along the experiment.

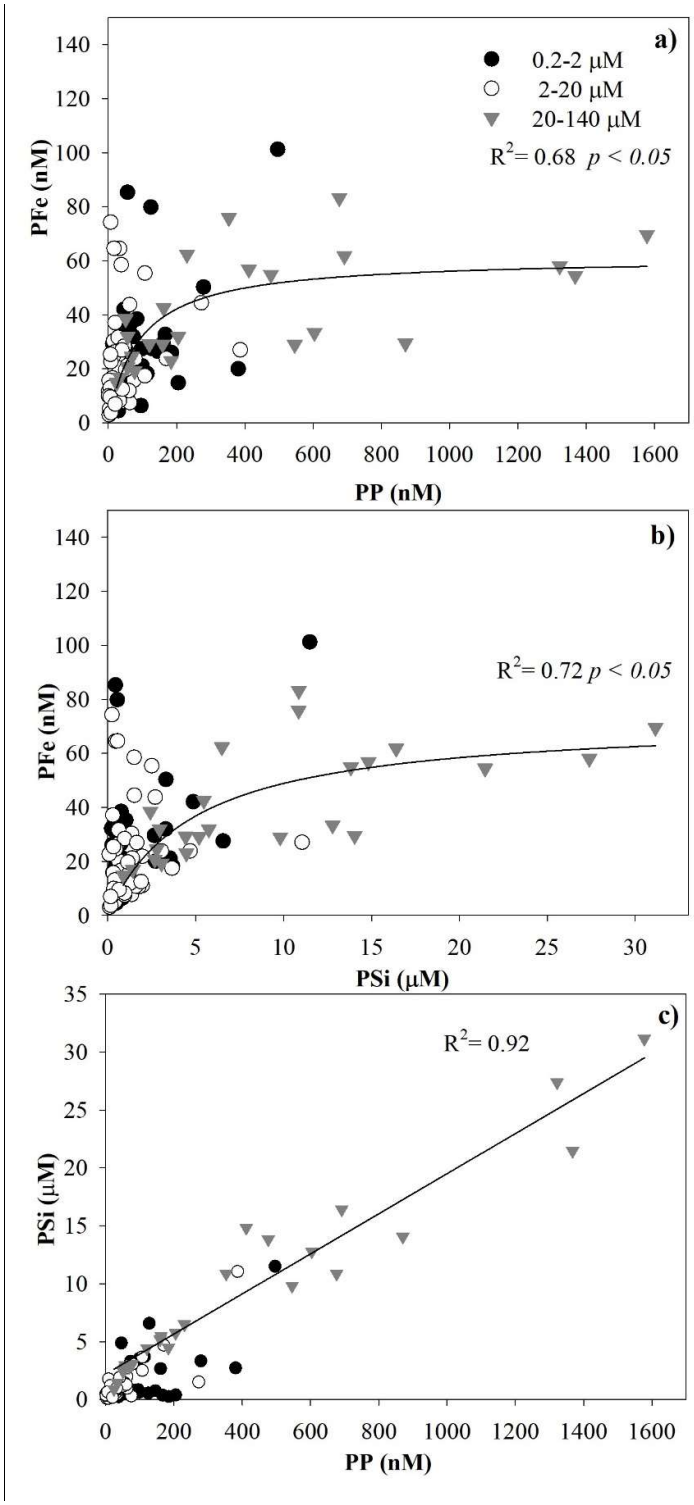

Figure 7. PFe (nM) versus particulate phosphorus (nM) (PFe:PP) (a), PFe versus particulate silicon (µM) (PFe:PSi) b) and particulate silicon (µM) versus particulate phosphorus (nM) (PFe:PP) c), for the three main size-class fractions (µm) in the brackish and seawater mesocosms.

enhanced NH_4^+ addition. This occurred regardless of initial differences in composition and abundance in the phytoplankton assemblages found in brackish and seawater. The pattern observed in all treatments over time, with the accumulation of Chl-a and POC, arguably responds to nutrient surplus and weakened top-down control. The latter could be explained by the zooplankton response, based on a probable low initial abundance in the water enclosures compared natural levels (Sánchez et al., 2011) and the time lag following rapid phytoplankton increase (Martin, 1965). The ultimate decline in Chl-a values and response variables, likely represented conditions of suppressed biological production. We observed accumulation of nutrients at highest NH_4^+ treatments (data not shown), suggesting possibility of a nutrient saturation. This could be result of inhibition of primary production by pH and/or limitation by inorganic carbon availability. Above pH 9, as was the case near the end of experiment, there is almost no CO_2, the bicarbonate starts to decrease, while only carbonate is accumulating (Hansen, 2002).

The converging response to nutrient surplus, was also observed in the measured variables and overall pattern in the highest NH_4^+ treatment. In the latter, the response followed the same trend as that exhibited in Conc 1 and Conc 2, but it was either similar or lower in magnitude. Hence some of the observed values of the different variables. With higher nutrient surplus, it was expected a larger biomass increase in Conc 3 relative to Conc 2. This could also partially be attributed to suppressed biological production, to the extent that a near two-fold NH_4^+ increase in Conc 3 seem to have produced a similar response in magnitude as Conc 2. Another possible factor involved, may have been the plankton community response to a significantly high nutrient input over a short period of time. Some studies have suggested that at NH_4^+ input >100 µM possible toxic effects could emerge (Olsen et al., 2006), whereas others showed that toxic effects begin only above 300 µM (Collos and Harrison, 2014). It is relevant to highlight that such nutrient increase over a short time window of the study, represent a situation unlikely to happen in the natural environment. Nonetheless, the response patterns observed reflect the underlying mechanism by which induced changes in the plankton assemblage, can play a significant role in iron dynamics.

4.1 Changes in the labile iron fraction over time

The observed correlation of both Fe labile fractions measured with the pattern of POC and Chl-a in both brackish and seawater, suggest a biological role affecting the distribution of iron. Decreasing concentrations of DFe_{Ch} concomitant with the increases in nutrient supply

316 can be attributed to direct uptake by a growing phytoplankton community. On the other hand,
317 the remarkably similar pattern of $TFe_{Ch,}$ POC and Chl-a, draws particular attention given that
318 it is conventionally the dissolved fraction the only considered to have a biological role. The
319 average increase of TFe_{Ch} of more than two-fold in both fractions, cannot be solely accounted
320 by decrease in DFe_{Ch}. This would imply an increase in Fe labile from a previously strongly
321 complexed Fe fraction that was not available to the chelex-100 resin. Presumably, the
322 increase could be result from induced physico-chemical changes by enhanced biological
323 activity. For instance, the release of organic ligands and/or exudates may have induced
324 changes in Fe speciation. The formation of colloids likely played a relevant role in the
325 observed changes between TFe_{Ch} and DFe_{Ch}. Encompassing a size range within the
326 boundaries of dissolved and particulate matter, colloids are subjected to possible bias via
327 artificial manipulation (Wells, 1998). Shifts between truly dissolved and truly particulate
328 chelex-labile fractions might not be perfectly reflected by DFe_{Ch} and TFe_{Ch} as these are
329 operationally defined classes. Moreover, colloid production rates can be enhanced by
330 biological action, presumably through a combination of cell exudation and lysis, microbial
331 degradation of particulate organic matter, sloppy feeding and excretion by zooplankton
332 (Wells and Goldberg, 1994). All these factors were gradually increased during the course of
333 the experiment due to nutrient addition. The results obtained here, as suggested by Frew et al.
334 (2006), supports the argument that PFe may be significantly more bioavailable.

335 A relevant factor related to the observed results was the high biomass attained in the
336 containers. Compared to concentrations of Chl-a and POC in the region (Iriarte et al., 2007,
337 González et al., 2010, González et al., 2011, Iriarte et al., 2012), high addition treatments in
338 the experiment reached much higher values. This contributed to formation of large
339 aggregates, visible to unaided eye. Possible results of this type of particle aggregation may
340 have been enhanced adsorption of dissolved forms onto aggregates and coagulation of
341 colloids. Both cases would result in transformation of a portion of the dissolved fraction into
342 particulate. In a mesoscale experiment, Wong et al. (2006) reported a quick transformation of
343 dissolved iron to particulate forms, with as much as 70% of the added iron transformed into
344 the non-dissolved form in less than 24 h. The mechanism alleged may involves combination
345 of biological uptake (Chen et al., 2003, Nodwell and Price, 2001) and simple adsorption of
346 dissolved (including colloidal) iron to the plankton cell surfaces as well as aggregation of
347 oxyhydroxides. Although Fe addition were not performed in this study, results in Wong et al.
348 (2006) illustrate possible mechanisms for Fe transformation. Finally, decrease in TFe_{Ch}

towards end of experiment following that of Chl-a and POC, would couple biological component to that of Fe cycling through settlement of senescent phytoplankton.

4.2 PFe: Biogenic versus lithogenic components

Total PFe and PFe values obtained from added size-fractionated data are not directly comparable given the different Sday of collection. Yet, The observed mismatch between these two measurements over time indicated probable methodological bias. PFe values obtained from added fractions may have caused potential overestimation due to possible compound errors of the procedure for each filter. Nonetheless, despite higher average values in added fractions, it can be argued that PFe values -obtained from size-fraction filtration- in time reflect the PFe trend observed in the corresponding treatment and therefore can still provide reliable information. PFe over time showed increments as expected, product of accumulation of newly formed organic biomass together with particle aggregation. Yet some concentrations reached may indicate that under high biological activity there was a probable contribution of Fe previously adsorbed on to containers walls during preconditioning.

PFe determination can be used as estimation of how much Fe is incorporated (intracellular) and adsorbed (extracellular) within planktonic community. Given that no reagent for removing adsorbed material from particle surfaces was used after sample filtration (Tovar-Sanchez et al., 2003), we can only provide an estimate of the total iron pool. The Fe:C ratio estimated here covered a broad range from 265 to 4224 $\mu mol:mol^{-1}$, with median values between 419 to 1430 and 753 to 1765 $\mu mol:mol^{-1}$ for brackish and seawater respectively. As a result of measuring the total iron pool, the values reported here are high above those reported previously in the literature for phytoplankton regarding the iron quota (2.3 to 370 $\mu mol:mol^{-1}$) (Sunda and Huntsman, 1995, Ho et al., 2003, Sarthou et al., 2005). Literature values of intracellular Fe range from 63 to 90% of total cellular Fe for different cell diameters and phytoplankton species (Sunda and Huntsman, 1995). Same study reported maximum intracellular Fe of 1700 $\mu mol:mol^{-1}$ for diatom species at high Fe conditions, 30 times higher than needed to support maximum growth rate. However, algal culture samples are dominated by biogenic Fe with little lithogenic Fe and therefore caution must be taken when comparing laboratory and natural samples (Frew et al., 2006), even more from coastal zones. Field studies (Frew et al., 2006, Hassler and Schoemann, 2009) from high nutrient low chlorophyll (HNLC) areas reported that extracellular iron (after chemical rinsing) accounted for 16 to 86% (mean ~ 50%) of total iron. Therefore, values reported here could potentially be reduced

by >50%. We then estimated total biogenic Fe (BFe), defined as the difference between total PFe and lithogenic (LFe). The latter is calculated by assuming all particulate Al (PAl) derives from lithogenic material and multiplying this term by the molar ratio (Fe:Al) of the abundance for upper continental crust (Martin et al., 1989). Average crustal ratios from literature of 0.19 (Wedepohl, 1995) and 0.33 (Taylor, 1964), would represent mean LFe fractions of ~49 % and ~71% respectively. Using the average value of these crustal ratios (0.27), mean BFe value obtained was 16 nM. This corresponds to an average of ~60% lower values from mean PFe measured here and supports that Fe:C estimated here could be further reduced, giving a range of 168 to 572 and 301 to 706 $\mu mol:mol^{-1}$ for brackish and seawater respectively. BFe derived from POC hence would represent ~40% of the measured PFe. It is therefore assumed that more than half of PFe had lithogenic origin, likely comprising several components from Fe-oxyhydroxides to refractory mineral phases (Frew et al., 2006). Part of LFe could be loosely bound to surface of phytoplankton cells or as colloidal form on particle aggregates (Hudson and Morel, 1989). Dominance of Fe from lithogenic origin is also observed in mean PFe:PAl ratio (0.39 and 0.29: n=158) obtained for brackish and seawater respectively (Fig. 8). Values obtained were near to the crustal ratio and close to values (Fe:Al) 0.36 from river sediment samples, south of the study site (Bertrand et al., 2012).

4.3 Fe-macronutrients ratios. PFe scavenging and particulate matter export

Control of trace metal scavenging by both sinking biogenic (Siddall et al., 2005) and lithogenic particles have relevant roles, of which the biogenic is regarded as the dominant process (Rogan et al., 2016). Biological parameters together with Fe fractions measured in this study, describe the role of biogenic particle scavenging, with the settling of organic matter during decline of the diatom bloom. As particle size plays the main role, smaller ones with larger surface to volume ratios, are likely to have a major role in adsorption of trace metals (Zhang et al., 2004). Yet, regarding fluxes of particulate material larger particles (> 53 µm) have a more significant role due to fast sinking rates (Lal, 1980, Anderson and Hayes, 2015), despite lower surface to volume ratio compared to the smaller fraction (0.2 - 53 µm).

The PFe values obtained here thus mainly represent the potential for Fe to be scavenged onto particle surfaces (extracellular) with a smaller fraction incorporated within phytoplankton. The exponential decrease in PFe:POC ratio observed with enhanced NH_4^+ addition, suggests a relation between increase in particulate matter size and surface availability. As biomass increases dominated by diatoms, volume to surface ratio of particulate matter decreases.

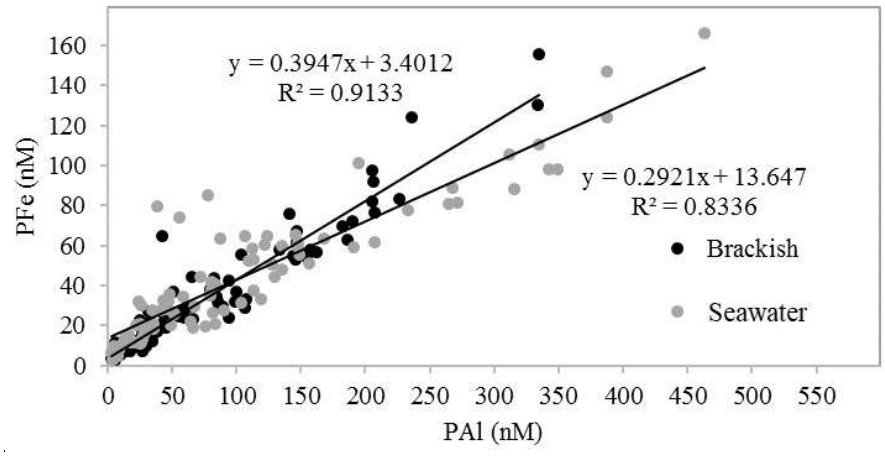

Figure 8. Distribution of particulate iron (PFe) versus particulate aluminum (PAl) (PFe:PAl) in the brackish and seawater mesocosms (n= 158, $R^2 = 0.82$).

Given that LFe was the dominant fraction, it can be argued that this extracellular form of iron drives the observed variation in PFe:PP ratio within 20-140 μm fraction. Despite sparse data, the combined measurements in brackish and seawater provide a significant correlation, describing a hyperbolic relation for PFe at increasing PP concentrations (Fig. 7). The PFe:PP ratio in this fraction for all treatments indicates that phytoplankton, more precisely diatoms, determined that the potential iron bound and scavenged, eventually levels off as the surface available decreases. Likewise, it highlights the role of diatoms as the main vector in scavenging of metals such as Fe. This relation is further observed in the PFe:PSi ratio, which contrasts with that of the macronutrients PSi and PP (Fig. 7c), that falls within Redfield ratio values, based on ~1 Si:N ratio (Brzezinski et al., 2003, Ho et al., 2003). Notwithstanding the low number of PFe size-fractionated measurements and that LFe accounted >50% of PFe, the data reflects the influence of the larger size-fraction (BFe) over the PFe distribution.

Accurate measurement of intracellular biogenic pool of Fe is required to provide the stoichiometric ratios of Fe with respect to biogenic macromolecules (C, N, and P) to incorporate Fe into the global biogeochemical models. It is therefore essential to determine the main factor(s) affecting particle export in the water column. Pico- and nano-plankton with a higher surface-to-volume ratios (Chisholm, 1992, Price et al., 1994) thrive in nitrogen recycled environments (NH_4^+), hence having lower Fe requirements. Conversely, diatoms from coastal assemblages have a higher requirement for iron (Bruland et al., 2001). Therefore, the observed shift to a diatom dominated community, particularly in brackish water, led to ratios of carbon and phosphorus to iron different of what would have been observed with a nano-plankton dominated community. Even though larger size of the diatoms may constrain amount of potential iron that can be adsorbed, the total surface area is likely be much higher in a diatom bloom. In addition, the rapid sinking rates of silica frustules make diatoms a more efficient vector for downward export of organic matter.

It is important to highlight that POC measurements include all organic carbon whether from autochthonous or allochthonous origin. The latter might be of particular relevance in fjord ecosystems subjected to constant input of terrigenous matter (Syvitski et al., 1987, Vargas et al., 2011). The input of marine organic carbon to surface sediments in northern Patagonia fjords varies widely accounting for 13 to 96% with an average of 61% (Sepúlveda et al., 2011). A study in Comau Fjord reports allochthonous contributions to the sediments of ~90 to ~24% at depths of 35 and 475 m, respectively (Silva et al., 2011). It is therefore relevant to highlight that such variability could have a significant effect on composition of water

collected. This is particularly relevant in the brackish water, where POC values were on average ~25% higher than seawater, hence decreasing the iron -to- carbon ratio. Chilean fjords constitute an important region for global burial of carbon (Silva et al., 2011), and therefore correct understanding of coupling of macro- and micro-nutrients is essential to determine the flux dynamics at continental margins in present and future scenarios.

CONCLUSIONS

The present study assessed how external nutrient input, such as of salmon aquaculture, can alter the pelagic community structure, indirectly affecting the biogeochemical cycling of Fe. Regardless of different community composition, the results in brackish and seawater showed similar trends, mainly determined by the enhanced NH_4^+ addition. Positively correlated changes in TFe_{Ch} with increase in NH_4^+ concentration, suggests that in addition to dissolvable Fe, changes in particulate labile fraction can also be linked to biological changes. Therefore, under certain conditions TFe_{Ch} should not be neglected as a potential bioavailable Fe source.

In presence of excess nutrients and dominance of micro-phytoplankton, observed changes in normalized ratios of phosphorus and carbon to iron, highlight the key role of phytoplankton assemblage composition in determining trace element dynamics. Furthermore, the changes highlight that measurement of all forms of Fe associated with phytoplankton *in situ* are relevant to estimate the role of biological pump in carbon and iron cycling. Given that promotion of diatom blooms result in more efficient downward export, and in consequence scavenged iron, raises the question of a potential increased role for iron in coastal productivity of certain regions in a future scenario of increased anthropogenic input of macronutrients and organic matter.

AKNOWLEDGEMENTS

This work was part of the project "CAN WASTE EMISSION FROM FISH FARMS CHANGE THE STRUCTURE OF MARINE FOOD WEBS (WAFOW)? - A comparative study of coastal ecosystems in Norway and Chile (project 193661), and the project A Cross-disciplinary Integrated Eco-system Eutrophication Research and Management Approach – CINTERA (project 216607), both funded by NTNU and the Norwegian Research Council.

476 This work was partially supported by CONICYT of the Chilean government, through the
477 FONDECYT research project (1110614). We would like to thank the scientists and staff of
478 the Fundacion San Ignacio del Huinay science station for their valuable support and the
479 logistics provided during sampling.

480 **REFERENCES**

481 ANDERSON, R. F. & HAYES, C. T. 2015. Characterizing marine particles and their impact
482 on biogeochemical cycles in the GEOTRACES program. Elsevier.
483 ARDELAN, M. V., HOLM-HANSEN, O., HEWES, C., REISS, C. S., SILVA, N.,
484 DULAIOVA, H., STEINNES, E. & SAKSHAUG, E. 2010. Natural iron enrichment
485 around the Antarctic Peninsula in the Southern Ocean. *Biogeosciences,* 7**,** 11–25.
486 ARRIGO, K. R. 2005. Marine microorganisms and global nutrient cycles. *Nature,* 437**,** 6.
487 BERTRAND, S., HUGHEN, K. A., SEPULVEDA, J. & PANTOJA, S. 2012. Geochemistry
488 of surface sediments from the fjords of Northern Chilean Patagonia (44–47 S): Spatial
489 variability and implications for paleoclimate reconstructions. *Geochimica et*
490 *Cosmochimica Acta,* 76**,** 125-146.
491 BRULAND, K. W., RUE, E. L. & SMITH, G. J. 2001. Iron and Macronutrients in California
492 Coastal Upwelling Regimes: Implications for Diatom Blooms. *Limnology and*
493 *Oceanography,* 46**,** 1661-1674.
494 BRZEZINSKI, M. A., DICKSON, M.-L., NELSON, D. M. & SAMBROTTO, R. 2003. Ratios
495 of Si, C and N uptake by microplankton in the Southern Ocean. *Deep Sea Research*
496 *Part II: Topical Studies in Oceanography,* 50**,** 619-633.
497 BUSCHMANN, A. H., RIQUELME, V. A., HERNÁNDEZ-GONZÁLEZ, M. C., VARELA,
498 D., JIMÉNEZ, J. E., HENRÍQUEZ, L. A., VERGARA, P. A., GUÍÑEZ, R. & FILÚN,
499 L. 2006. A review of the impacts of salmonid farming on marine coastal ecosystems in
500 the southeast Pacific. *ICES Journal of Marine Science: Journal du Conseil,* 63**,** 1338-
501 1345.
502 CHEN, M., DEI, R. C. H., WANG, W. X. & GUO, L. 2003. Marine diatom uptake of iron
503 bound with natural colloids of different origins. *Marine Chemistry,* 81**,** 177-189.
504 CHISHOLM, S. W. 1992. Phytoplankton size. *Primary productivity and biogeochemical*
505 *cycles in the sea. Plenum***,** 213-237.
506 CLOERN, J. E. 2001. Our evolving conceptual model of the coastal eutrophication problem.
507 *Marine Ecology Progress Series,* 210**,** 53.
508 COLLOS, Y. & HARRISON, P. J. 2014. Acclimation and toxicity of high ammonium
509 concentrations to unicellular algae. *Marine pollution bulletin,* 80**,** 8-23.
510 DE BAAR, H. J. & DE JONG, J. T. 2001. Distributions, sources and sinks of iron in seawater.
511 *IUPAC series on analytical and physical chemistry of environmental systems,* 7**,** 123-
512 254.
513 FIELD, C. B., BEHRENFELD, M. J., RANDERSON, J. T. & FALKOWSKI, P. 1998. Primary
514 production of the biosphere: integrating terrestrial and oceanic components. *Science,*
515 281**,** 237-240.
516 FREW, R. D., HUTCHINS, D. A., NODDER, S., SANUDO-WILHELMY, S., TOVAR-
517 SANCHEZ, A., LEBLANC, K., HARE, C. E. & BOYD, P. W. 2006. Particulate iron
518 dynamics during FeCycle in subantarctic waters southeast of New Zealand. *Global*
519 *Biogeochemical Cycles,* 20.
520 GONZÁLEZ, H. E., CALDERÓN, M., CASTRO, L., CLÉMENT, A., CUEVAS, L.,
521 DANERI, G., IRIARTE, J., LIZÁRRAGA, L., MARTÍNEZ, R. & MENSCHEL, E.

2010. Primary production and plankton dynamics in the Reloncaví Fjord and the Interior Sea of Chiloé, Northern Patagonia, Chile. *Marine Ecology Progress Series,* 402**,** 13-30.

GONZÁLEZ, H. E., CASTRO, L., DANERI, G., IRIARTE, J., SILVA, N., VARGAS, C., GIESECKE, R. & SÁNCHEZ, N. 2011. Seasonal plankton variability in Chilean Patagonia fjords: Carbon flow through the pelagic food web of Aysen Fjord and plankton dynamics in the Moraleda Channel basin. *Continental Shelf Research,* 31**,** 225-243.

HANSEN, P. J. 2002. Effect of high pH on the growth and survival of marine phytoplankton: implications for species succession. *Aquatic microbial ecology,* 28**,** 279-288.

HASSLER, C. S. & SCHOEMANN, V. 2009. Discriminating between intra- and extracellular metals using chemical extractions: an update on the case of iron. *Limnology and Oceanography: Methods,* 7**,** 479-489.

HO, T. Y., QUIGG, A., FINKEL, Z. V., MILLIGAN, A. J., WYMAN, K., FALKOWSKI, P. G. & MOREL, F. M. M. 2003. The elemental composition of some marine phytoplankton. *Journal of Phycology,* 39**,** 1145-1159.

HUDSON, R. J. & MOREL, F. M. 1989. Distinguishing between extra-and intracellular iron in marine phytoplankton. *Limnology and Oceanography***,** 1113-1120.

HÄUSSERMANN, V. & FÖRSTERRA, G. 2009. Marine benthic fauna of Chilean Patagonia. *Nature in Focus, Santiago*.

IRIARTE, J. L., GONZÁLEZ, H., LIU, K., RIVAS, C. & VALENZUELA, C. 2007. Spatial and temporal variability of chlorophyll and primary productivity in surface waters of southern Chile (41.5-43 S). *Estuarine, Coastal and Shelf Science,* 74**,** 471-480.

IRIARTE, J. L., KUSCH, A., OSSES, J., RUIZ, M. & IRIARTE, J. L. 2001. Phytoplankton biomass in the sub-Antarctic area of the Straits of Magellan (53 S), Chile during spring-summer 1997/1998. *Polar Biology,* 24**,** 154-162.

IRIARTE, J. L., PANTOJA, S., GONZÁLEZ, H., SILVA, G., PAVES, H., LABBÉ, P., REBOLLEDO, L., ARDELAN, M. & HÄUSSERMANN, V. 2013. Assessing the micro-phytoplankton response to nitrate in Comau Fjord (42°S) in Patagonia (Chile), using a microcosms approach. *Environmental Monitoring and Assessment,* 185**,** 5055-5070.

IRIARTE, J. L., PANTOJA, S., GONZÁLEZ, H. E., SILVA, G., PAVES, H., LABBÉ, P., REBOLLEDO, L., VAN ARDELAN, M. & HÄUSSERMANN, V. 2012. Assessing the micro-phytoplankton response to nitrate in Comau Fjord (42° S) in Patagonia (Chile), using a microcosms approach. *Environmental Monitoring and Assessment***,** 1-16.

JANTZEN, C., HÄUSSERMANN, V., FÖRSTERRA, G., LAUDIEN, J., ARDELAN, M., MAIER, S. & RICHTER, C. 2013. Occurrence of a cold-water coral along natural pH gradients (Patagonia, Chile). *Marine biology,* 160**,** 2597-2607.

LAL, D. 1980. Comments on some aspects of particulate transport in the oceans. *Earth and Planetary Science Letters,* 49**,** 520-527.

MAGAZZÙ, G., PANELLA, S. & DECEMBRINI, F. 1996. Seasonal variability of fractionated phytoplankton, biomass and primary production in the Straits of Magellan. *Journal of Marine Systems,* 9**,** 249-267.

MARTIN, J. H. 1965. PHYTOPLANKTON-ZOOPLANKTON RELATIONSHIPS IN ARRAGANSETT BAY. *Limnology and Oceanography,* 10**,** 185-191.

MARTIN, J. H., GORDON, R. M., FITZWATER, S. & BROENKOW, W. W. 1989. VERTEX: phytoplankton/iron studies in the Gulf of Alaska. *Deep Sea Research Part A. Oceanographic Research Papers,* 36**,** 649-680.

MOREL, F. M. M. & PRICE, N. 2003. The biogeochemical cycles of trace metals in the oceans. *Science,* 300**,** 944-947.
NODWELL, L. M. & PRICE, N. M. 2001. Direct use of inorganic colloidal iron by marine mixotrophic phytoplankton. *Limnology and Oceanography***,** 765-777.
OLSEN, L. M., HERNÁNDEZ, K. L., VAN ARDELAN, M., IRIARTE, J. L., SÁNCHEZ, N., GONZÁLEZ, H. E., TOKLE, N. & OLSEN, Y. 2014. Responses in the microbial food web to increased rates of nutrient supply in a southern Chilean fjord: possible implications of cage aquaculture. *Aquaculture Environment Interactions,* 6**,** 11-27.
OLSEN, Y., AGUSTÍ, S., ANDERSEN, T., DUARTE, C. M., GASOL, J. M., GISMERVIK, I., HEISKANEN, A. S., HOELL, E., KUUPPO, P. & LIGNELL, R. 2006. A comparative study of responses in planktonic food web structure and function in contrasting European coastal waters exposed to experimental nutrient addition. *Limnology and Oceanography***,** 488-503.
OLSEN, Y., OLSEN, L. & TSUKAMOTO, K. Environmental impact of aquaculture on coastal planktonic ecosystems. Fisheries for global welfare and environment. Memorial book of the 5 th World Fisheries Congress 2008, 2008. TERRAPUB, Tokyo(Japan).
PARSONS, T. R. M. & LALLI, Y. 1984. A manual of chemical and biological methods for seawater analysis.
PICKARD, G. 1971. Some physical oceanographic features of inlets of Chile. *Journal of the Fisheries Board of Canada,* 28**,** 1077-1106.
PRICE, N. M., AHNER, B. & MOREL, F. 1994. The equatorial Pacific Ocean: Grazer-controlled phytoplankton populations in an iron-limited ecosystem. *Limnology and Oceanography***,** 520-534.
REDFIELD, A. C. 1958. The biological control of chemical factors in the environment. *American scientist,* 46**,** 230A-221.
ROGAN, N., ACHTERBERG, E. P., LE MOIGNE, F. A., MARSAY, C. M., TAGLIABUE, A. & WILLIAMS, R. G. 2016. Volcanic ash as an oceanic iron source and sink. *Geophysical Research Letters,* 43**,** 2732-2740.
SÁNCHEZ, N., GONZÁLEZ, H. E. & IRIARTE, J. L. 2011. Trophic interactions of pelagic crustaceans in Comau Fjord (Chile): their role in the food web structure. *Journal of Plankton Research,* 33**,** 1212-1229.
SARTHOU, G., TIMMERMANS, K. R., BLAIN, S. & TRÉGUER, P. 2005. Growth physiology and fate of diatoms in the ocean: a review. *Journal of Sea Research,* 53**,** 25-42.
SEPÚLVEDA, J., PANTOJA, S. & HUGHEN, K. A. 2011. Sources and distribution of organic matter in northern Patagonia fjords, Chile (~ 44–47° S): A multi-tracer approach for carbon cycling assessment. *Continental Shelf Research,* 31**,** 315-329.
SIDDALL, M., HENDERSON, G. M., EDWARDS, N. R., FRANK, M., MÜLLER, S. A., STOCKER, T. F. & JOOS, F. 2005. 231 Pa/230 Th fractionation by ocean transport, biogenic particle flux and particle type. *Earth and Planetary Science Letters,* 237**,** 135-155.
SILVA, N., CALVETE, C. & SIEVERS, H. 1998. Masas de agua y circulación general para algunos canales australes entre Puerto Montt y Laguna San Rafael, Chile (Crucero Cimar-Fiordo 1). *Cienc. Tecnol. Mar,* 21**,** 17-48.
SILVA, N. & PREGO, R. 2002. Carbon and nitrogen spatial segregation and stoichiometry in the surface sediments of southern Chilean inlets (41–56 S). *Estuarine, Coastal and Shelf Science,* 55**,** 763-775.
SILVA, N., VARGAS, C. A. & PREGO, R. 2011. Land–ocean distribution of allochthonous organic matter in surface sediments of the Chiloé and Aysén interior seas (Chilean Northern Patagonia). *Continental Shelf Research,* 31**,** 330-339.

SOTO, D. & NORAMBUENA, F. 2004. Evaluation of salmon farming effects on marine systems in the inner seas of southern Chile: a large-scale mensurative experiment. *Journal of Applied Ichthyology,* 20**,** 493-501.

STRAIN, P. & HARGRAVE, B. 2005. Salmon aquaculture, nutrient fluxes and ecosystem processes in southwestern New Brunswick. *Environmental Effects of Marine Finfish Aquaculture.* Springer.

SUNDA & HUNTSMAN, S. A. 1995. Iron uptake and growth limitation in oceanic and coastal phytoplankton. *Marine Chemistry,* 50**,** 189-206.

SYVITSKI, J. P., BURRELL, D. C. & SKEI, J. M. 1987. Fjords: processes and products.

TAYLOR, S. 1964. Abundance of chemical elements in the continental crust: a new table. *Geochimica et cosmochimica acta,* 28**,** 1273-1285.

TOVAR-SANCHEZ, A., SAÑUDO-WILHELMY, S. A., GARCIA-VARGAS, M., WEAVER, R. S., POPELS, L. C. & HUTCHINS, D. A. 2003. A trace metal clean reagent to remove surface-bound iron from marine phytoplankton. *Marine Chemistry,* 82**,** 91-99.

UTHERMOHL, H. 1958. Zur vervollkommnung der quantitativen phytoplankton methodic. *Mitt. Int. Verein. Theor. Andew. Limnolgie,* 9**,** 1-38.

VARGAS, C. A., MARTINEZ, R. A., SAN MARTIN, V., AGUAYO, M., SILVA, N. & TORRES, R. 2011. Allochthonous subsidies of organic matter across a lake-river-fjord landscape in the Chilean Patagonia: Implications for marine zooplankton in inner fjord areas. *Continental Shelf Research,* 31**,** 187-201.

WANG, W. X., DEI, R. C. H. & XU, Y. 2001. Cadmium uptake and trophic transfer in coastal plankton under contrasting nitrogen regimes. *Marine Ecology Progress Series,* 211**,** 293-298.

WEDEPOHL, K. H. 1995. The composition of the continental crust. *Geochimica et cosmochimica Acta,* 59**,** 1217-1232.

WELLS, M. L. 1998. Marine colloids: A neglected dimension. *Nature,* 391**,** 530-531.

WELLS, M. L. & GOLDBERG, E. D. 1994. The Distribution of Colloids in the North Atlantic and Southern Oceans. *Limnology and Oceanography,* 39**,** 286-302.

WONG, C. S., JOHNSON, W. K., SUTHERLAND, N., NISHIOKA, J., TIMOTHY, D. A., ROBERT, M. & TAKEDA, S. 2006. Iron speciation and dynamics during SERIES, a mesoscale iron enrichment experiment in the NE Pacific. *Deep Sea Research Part II: Topical Studies in Oceanography,* 53**,** 2075-2094.

ZHANG, L., CHEN, M., YANG, W., XING, N., LI, Y., QIU, Y. & HUANG, Y. 2004. Size-fractionated thorium isotopes (228 Th, 230 Th, 232 Th) in surface waters in the Jiulong River estuary, China. *Journal of environmental radioactivity,* 78**,** 199-216.

ÖZTÜRK, M., STEINNES, E. & SAKSHAUG, E. 2002. Iron Speciation in the Trondheim Fjord from the Perspective of Iron Limitation for Phytoplankton. *Estuarine, Coastal and Shelf Science,* 55**,** 197-212.